Measuring stacking fault densities in shock-compressed FCC crystals using *in situ* x-ray diffraction

2006 J. Phys.: Condens. Matter 18 6749

(http://iopscience.iop.org/0953-8984/18/29/014)

INSTITUTE OF PHYSICS PUBLISHING JOURNAL OF PHYSICS: CONDENSED MATTER

J. Phys.: Condens. Matter **18** (2006) 6749–6757 doi:10.1088/0953-8984/18/29/014

Measuring stacking fault densities in shock-compressed FCC crystals using *in situ* x-ray diffraction

K Rosolankova[1], J S Wark[1], E M Bringa[2] and J Hawreliak[2]

[1] Department of Physics, Clarendon Laboratory, University of Oxford, Oxford OX1 3PU, UK
[2] Lawrence Livermore National Laboratory, Livermore, CA 94550, USA

Received 21 April 2006
Published 30 June 2006
Online at stacks.iop.org/JPhysCM/18/6749

Abstract

A method is presented of *in situ* measurements of stacking fault densities in shocked face-centred-cubic (FCC) crystals using x-ray diffraction. Using results from both the second and fourth diffraction orders, wherein shifts in the Bragg peaks due to faulting are accounted for, we calculated fault densities present in a molecular dynamics (MD) simulation of shocked single crystal of copper. The results are in good quantitative agreement with dislocation density measurements inferred directly from the MD simulation. The x-ray diffraction method thus presents a real possibility for experimental determination in real time of dislocation densities in crystals during shock wave passage.

1. Introduction

For several decades, time-dependent *in situ* x-ray diffraction has been used as a tool for studying the structure of crystals under shock loading, enabling material investigation at the lattice level on extremely short (nano- and picosecond) timescales [1–9]. X-rays are scattered from the atoms in a crystal and interfere constructively when the well-known Bragg condition is satisfied:

$$\lambda = 2d_{hkl} \sin\theta_{\mathrm{B}}, \tag{1}$$

where λ is the x-ray wavelength, θ_{B} is the Bragg angle between the diffracted signal and the planes defined by indices (hkl), and d_{hkl} is the spacing of the crystal planes labelled by these indices.

Elastic strains in a crystal cause angular shifts in the diffracted radiation peaks. Under the assumption of zero plastic dilatation, an x-ray diffraction measurement of the average transverse and longitudinal elastic strains in a material therefore provides quantitative information about the plastic strains under conditions of uniaxial strain.

In certain pressure regimes, the rate of plastic flow in a crystalline material subjected to uniaxial shock loading is directly related to the presence and movement of dislocations within it (we ignore here, for example, plastic flow related to twinning). The rate at which a material undergoes plastic strain, $\dot{\epsilon}_{\mathrm{p}}$, is determined by the well-known equation due to Orowan [10],

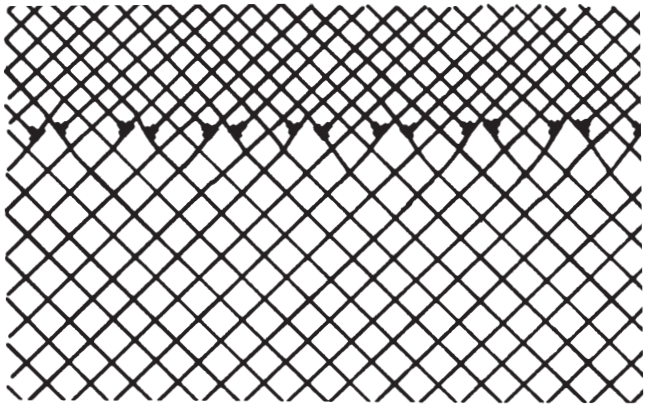

Figure 1. Interface formed by dislocations at the shock front, moving from top to bottom in the figure, as modelled by Smith [12]. The formed dislocations relieve shear stress in the material and a cubic lattice with a reduced unit cell size is formed behind the shock front.

which provides the following relationship between $\dot{\epsilon_{\mathrm{p}}}$ and the density of the mobile dislocations, ρ_{m}, the magnitude of their Burgers vector, b, and their mean speed $\langle v \rangle$:

$$\dot{\epsilon_{\mathrm{p}}} = b\rho_{\mathrm{m}}\langle v \rangle. \tag{2}$$

The high plastic strain rates observed in materials clearly indicate that dislocation densities within shocked samples can be extremely high. Recent *in situ* x-ray diffraction experiments have shown that a Cu sample shocked on timescales shorter than a nanosecond approaches the hydrostat, with lateral plastic strains of several per cent [8, 11]. Even assuming that the maximum dislocation velocity is the local speed of sound, dislocation densities must exceed 10^{11} cm^{-2}, and would be much higher for lower dislocation velocities and large strain rates. Taking into account the fact that the observed strain rates in the above-referenced experiments were lower bounds, experimental evidence of this nature points towards possible dislocation densities in excess of 10^{12} cm^{-2}, a conclusion which, as will be shown later, is borne out by large-scale molecular dynamics (MD) calculations.

In order to put this work into an historical context, it is important to note that we are only now, with the development of MD simulations, beginning to come to a detailed understanding of the nature of shock-induced plasticity at the lattice level.

One of the first models that attempted to describe the behaviour of a cubic lattice under shock conditions was proposed by Smith [12] (figure 1). In this model, edge dislocations are produced at the shock front, and move (supersonically) along with the front, allowing compression in all directions behind it. The model was later modified by Meyers [13, 14], who proposed lower dislocation velocities, with a continuing production of layers of dislocations within the crystal behind the shock front. In both these models, the edge dislocations created at the front move in order to accommodate the high shear stresses caused by the shock wave to which the crystal is subjected. They form an interface between the shocked and unshocked regions in the crystal, which are both cubic, with the lattice in the shocked region having a reduced unit cell size. The Meyers' model also predicts large dislocation densities, similar in number to those referred to above.

More recently, large-scale multi-million-atom MD simulations have shed new light on the possible mechanisms occuring in shocked crystals. In the seminal work of Holian and co-workers [15], it was shown that high densities of stacking faults could be generated at the shock front of a FCC crystal, relieving the shear stress. Similar conclusions have been reached in

more recent work which we use here, involving even larger numbers of atoms and pre-existing dislocations [16].

However, it is important to note that, despite the inference from Orowan's equation that experimentally determined strain rates require large dislocation densites, and the confirmations of MD simulations which corroborate such a conclusion, no *direct* experimental evidence for such high dislocation densities exists to date. Recovered samples consistently display dislocation density orders of magnitude smaller than those referred to above [14, 17]. It is presumed that the reason for this is the reaction between and mutual annihilation of dislocations of opposing signs upon shock release. However, as this has never been shown experimentally, there clearly remains a pressing need to develop *in situ* diagnostics of dislocation densities, in order to verify these models and fundamental assumptions experimentally.

Stacking faults in FCC crystals, such as copper, are known to introduce angular shifts in the intensity peaks of x-ray diffraction scattered from the material in addition to the shifts due to changes in lattice spacing. The magnitude and direction of the fault-induced shift depend on the Miller indices (hkl) of the diffracting planes [9, 18, 19]. Thus, as pointed out by Zaretsky [19], *in situ* x-ray diffraction offers a potential method of directly measuring stacking fault densities within a shocked solid.

That said, the dislocation densities of interest within shocked solid are far greater than those found in static samples, and MD simulations further indicate large elastic distortions of the lattice between dislocations. It is therefore pertinent to ask whether such shifts could possibly be observed in a shocked sample? In order to take the first steps in answering this question, and to motivate experimental work in this area, we have taken the output of a large-scale MD model, and post-processed the data in order to obtain simulated x-ray diffraction patterns. We then determined the positions of the peaks in the diffracted radiation, and used the positions of peaks of differing Miller indices to infer stacking fault densities. The stacking fault densities thus inferred are compared with those deduced simply from counting faults by the colour coding of atoms according to their coordination number. As we shall show, good agreement is found, pointing towards a real possibility of *in situ* experimental measurement of dislocation concentrations in shocked materials.

2. Theory

The presence of stacking faults in a crystal causes a shift in the phase of the incident and scattered x-rays with respect to the lattice, which in turn alters the resultant Bragg peak position [18]. This shift in the Bragg peak is additional to the shift due to the change in the mean lattice spacing due to shock compression. The expressions for the stacking-fault induced angular Bragg peak shifts in radians, $\Delta(2\theta)$, for reflections from {200} and {400} planes in a FCC crystal are:

$$\Delta(2\theta)_{200} = -\frac{\sqrt{3}\alpha \tan\theta_{200}}{4\pi}, \qquad \Delta(2\theta)_{400} = +\frac{\sqrt{3}\alpha \tan\theta_{400}}{8\pi}, \tag{3}$$

where $1/\alpha$ is the average number of planes between two consecutive stacking faults.

The diffraction angle θ is related to the magnitude of the diffraction vector G via the expression

$$\sin\theta = \frac{G}{2k}. \tag{4}$$

Combining the derivative of this expression with equation (3) gives the respective shifts in the second-and fourth-order peaks in k-space due to the stacking faults as

$$dG_{200} = -\frac{\sqrt{3}G_{200}\alpha}{8\pi}, \qquad dG_{400} = +\frac{\sqrt{3}G_{400}\alpha}{16\pi}. \tag{5}$$

Since an x-ray diffraction measurement is equivalent to taking a Fourier transform of the lattice, equation (5) provides the shifts, solely due to the presence of dislocations in the material, in the positions of the points in k-space. (It should be noted that this expression is one-dimensional, i.e. in the second order, the shift of the peak corresponding to point (200) in k-space will be along the k_x direction only, for the (020) peak the shift will be along k_y etc. The same is true for the fourth-order diffraction.)

Now, as well as the shifts in diffraction due to the stacking faults, the peaks will move in k-space due to compression of the lattice by the shock (in the presence of plastic flow, there is elastic strain within the lattice in all three orthogonal directions). In this paper we consider the influence of these stacking faults on diffraction from shocked single crystals, as have been used previously in nanosecond resolution diffraction experiments [8]. Let us define the position of, say, the (200) peak in k-space in the absence of stacking faults (but taking account of elastic compression), as $2A$, and thus that of the (400) peak is $4A$. We denote by |200| and |400| the actual respective k_x-component of the distances from the origin in k-space of the (200) and (400) reflections. The positions of the diffraction peaks in k-space can then be rewritten in the form:

$$|200| = 2A - \frac{A\sqrt{3}\alpha}{4\pi}, \qquad |400| = 4A + \frac{A\sqrt{3}\alpha}{4\pi}. \tag{6}$$

Similar expressions follow for orthogonal directions in k-space. As A represents the theoretical position of the first-order diffraction peak, in reality forbidden in FCC crystals, discounting the dislocation-induced shift of the x-ray diffraction peaks, the values of A inferred from equation (6) for points which, in the uncompressed crystal, lie at (100), (010), and (001) in k-space are the corners of the 'corrected' first-order inverse unit cell. Thus the values of A for the directions in k_x, k_y and k_z can be used to determine the volumetric compression as deduced from diffraction, a strain which should agree with the atomic density rise in the sample due to the shock-induced compression of the material.

Eliminating A from the expressions in equation (6), we then find that the probability of the occurrence of a stacking fault between any two consecutive planes, α, is given by:

$$\alpha = \frac{8\pi(|400| - 2|200|)}{\sqrt{3}(|400| + |200|)}. \tag{7}$$

This is related to the dislocation density, ρ_{d}:

$$\rho_{\mathrm{d}} = (\alpha/l)^2, \tag{8}$$

where l is the separation of two consecutive planes in the crystal.

3. Simulations

A computational x-ray diffraction tool for calculating three-dimensional (3D) Fourier transforms (FT) was developed for post-processing of MD simulations of shock-compressed crystals. The use of 3D FT provides better accuracy in comparison with one-dimensional (1D) or two-dimensional (2D) FT.

The output from an MD simulation of a shocked single copper crystal containing 256×10^6 atoms was studied [16]. Its dimensions prior to shock launch were $200 \times 200 \times 1600$ unit cells, with the long side of the sample along the shock propagation direction [001], and the unperturbed unit cell size $a_0 = 3.615$ Å. The simulation thus spanned 0.6 μm in length. In

terms of the unit cell positions, the location of the centre of the crystal prior to shock launch was at (0, 0, 0) along the three primary axes. In other words, the limits of the crystal, in terms of the unit cells, were −100 and +100 for both [100] and [010] directions, and −800 and +800 for the [001] direction.

Two prismatic loops were incorporated into the crystal prior to shock launch. The first one was located at ∼0.18 μm and the second one at ∼0.4 μm along the z axis, corresponding to unit cell positions of ∼−320 and ∼230, respectively. The shock wave launched in the crystal had a 50 ps long linear ramp. The peak pressure generated was 35 GPa, exceeding the thresholds for homogeneous and inhomogeneous dislocation generation of ∼32 and ∼10 GPa, respectively. The total duration of the simulation was ∼130 ps. The simulation studied was therefore a complicated system enhanced with features such as the embedded defects and the linear ramp, in order to faithfully represent a real experimental crystal sample. Further details of this particular simulation can be found in the work of Bringa [16].

3.1. Results

A snapshot of the atomic positions was taken from the MD simulation at a time of 125 ps after the start of the simulation. By this time the foot of the ramp had traversed nearly 700 unit cells, and the ramp, originally of 50 ps duration, had steepened considerably. For this particular output in time, the 3D FT of the atomic positions was calculated for various regions of the crystal along its length, and the weighted centres of intensity for the Bragg peaks (both second and fourth order) were determined. The positions of the peaks can be used to infer the lattice spacing, and hence compression. The results of this analysis, at this stage *without* taking into account possible shifts in the Bragg peaks due to the stacking faults, are shown in figure 2.

In this figure, the shock has propagated from left to right. We show the elastic strains in the crystal along the length of the crystal inferred from the positions of simulated diffraction peaks. Note that the strain in the shock propagation direction (z direction) is larger than the strain in the orthogonal directions, i.e. the material is not compressed in a fully hydrostatic manner. Nonetheless, significant plastic flow must have taken place to give rise to the elastic strains in the orthogonal directions (in these directions, the elastic and plastic strains should be equal and opposite).

It is not our intention to go into a full analysis of the mechanisms and rate of plasticity in this particular simulation, as that is covered in the work of Bringa and co-workers [16]. However, what should be noted from figure 2 is that the volumetric strain inferred from the Bragg peak positions in the three principal directions in k-space (again, we emphasize that this is neglecting the effect of dislocations) does not entirely agree with the compression of the crystal gleaned from the MD simply by calculating the atomic density in a given region of the sample by counting the number of atoms in a unit of volume. Indeed, it can be seen that the compression inferred from the x-ray peak positions is less than that given by the atomic density calculation in the case of second-order diffraction, but greater than for fourth-order diffraction. Also, note that the discrepancy between the compression inferred from diffraction simulation and atomic density calculation is least at the shock front (where the plastic flow must be least, as there is little strain orthogonal to the propagation direction), and greatest at the left-hand boundary—a region where, as we shall see later, plastic flow is largely due to homogeneous dislocation generation.

As shown above, the positions of the second-and fourth-order peaks can be used to derive both A, the theoretical first-order diffraction peak position taking into account the presence of dislocations, and α, the probability of stacking fault occurrence between two consecutive atomic planes. A measurement of A in the three orthogonal directions provides

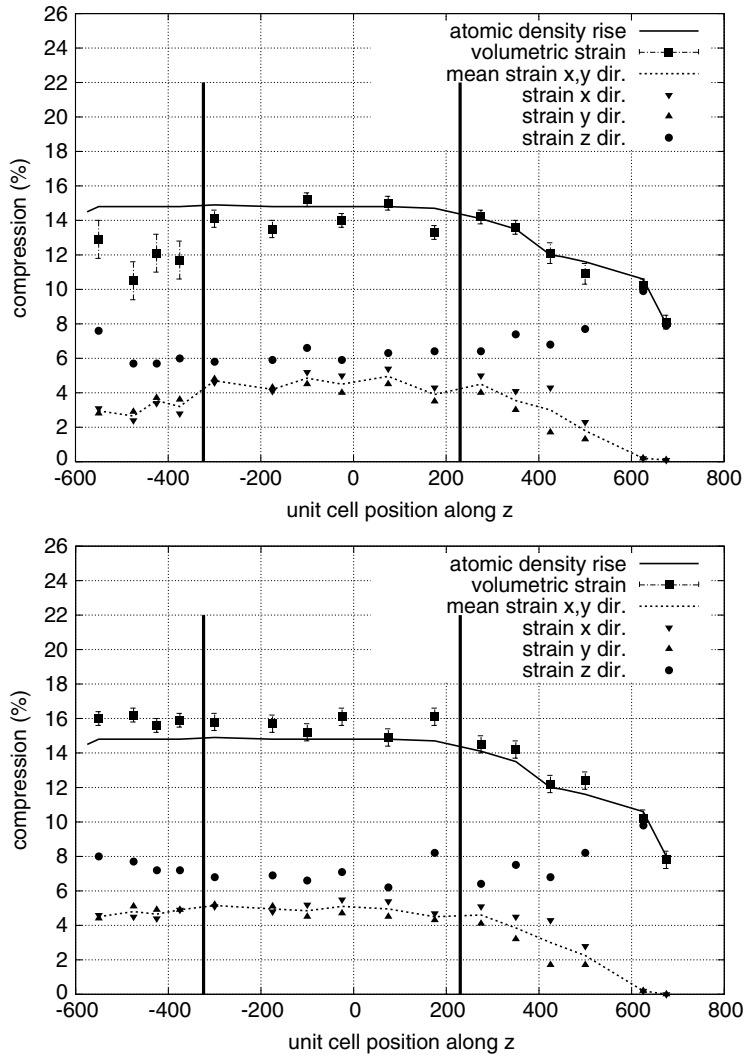

Figure 2. Second-order (top) and fourth-order (bottom) results of simulated x-ray diffraction. Volumetric compression of sampled cubic sections can be compared with atomic density rise. Two vertical lines mark the original positions of the two prismatic loops. The shock propagates from left to right, with the shock front at $z = +675$.

the measurement of crystal compression after taking into account shifts in the peak due to the dislocation densities.

For the sample analysed here, the corrected compressions calculated using equation (7) are shown in figure 3. Once the fault-induced shifts in the diffraction peaks have been accounted for, excellent agreement between the x-ray diffraction results and the atomic density rise is reached for all regions of the crystal.

3.2. Dislocation densities

Dislocation densities calculated using equation (8) are shown in figure 4. Note that the inferred dislocation density is highest to the left of the crystal, reaching values of order $\sim 2 \times 10^{13}$ cm^{-2},

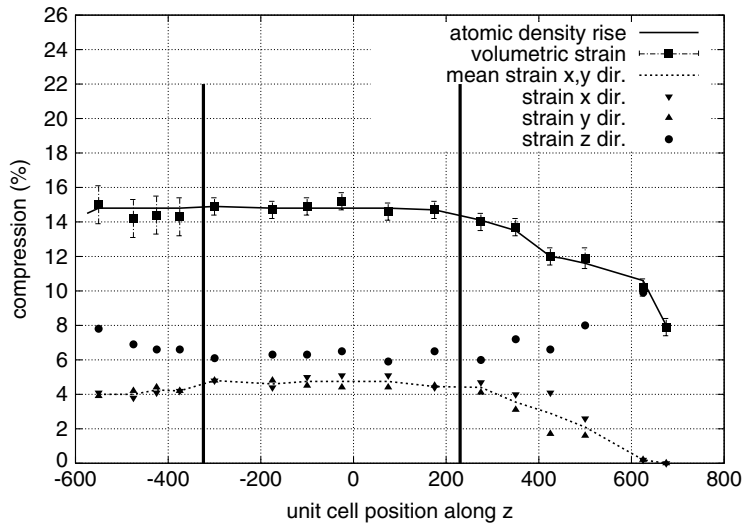

Figure 3. Corrected 1D and volumetric strains in sampled cubic sections of Cu simulation.

with an approximately three-fold decrease in density once the compression wave has passed the first prismatic loop. Shown alongside the dislocation densities inferred from the shifts of the diffraction lines are the densities obtained by directly counting dislocations within the image of the simulation. Certain parts of the crystal between the prismatic loops, near unit cell positions $z = -100$ and $+75$, have significantly lower dislocation densities than regions ahead of and behind them. X-ray diffraction post-processing yielded volumetric compressions coinciding with the atomic density rise in both second-and fourth-order calculations in these crystal regions (figure 2). The stacking fault densities were clearly too low to induce any significant shifts in the diffraction peaks. As such, the errors on the inferred values of α and dislocation densities are too large for the results to have any quantitative validity. For this reason, Figure 4 omits the values of dislocation density at these points. The horizontal line marked on the graph indicates the cut-off dislocation density value, which can still be considered quantitatively accurate (i.e. at least from this MD simulation, our error bars are too high to detect dislocation densities below this value).

A snapshot of the dislocations is also shown in figure 4. This image is obtained by noting that atoms within the stacking faults have a different centro-symmetry parameter than the FCC material [20]. This image shows only those atoms present within such stacking faults. The dislocation density can then be found directly simply by counting the number of faults crossing unit area. We note that the agreement between the dislocation density inferred from diffraction and that obtained directly is good—within approximately a factor of two. Both methods show a higher concentration of dislocations on the left-hand side of the sample, with a reduction once the first prismatic loop is reached.

A detailed analysis of the physics behind the changes in dislocation density across this sample will be presented in the work of Bringa [16]—we give a brief explanation here only for the sake of completeness, as the main purpose of this work is to show the consistency between the diffraction approach and the direct counting method. This sample is being compressed by a ramped pressure pulse. Within perfect crystals, once the theoretical shear strength of the material is reached, a high density of dislocations is generated homogeneously at the shock

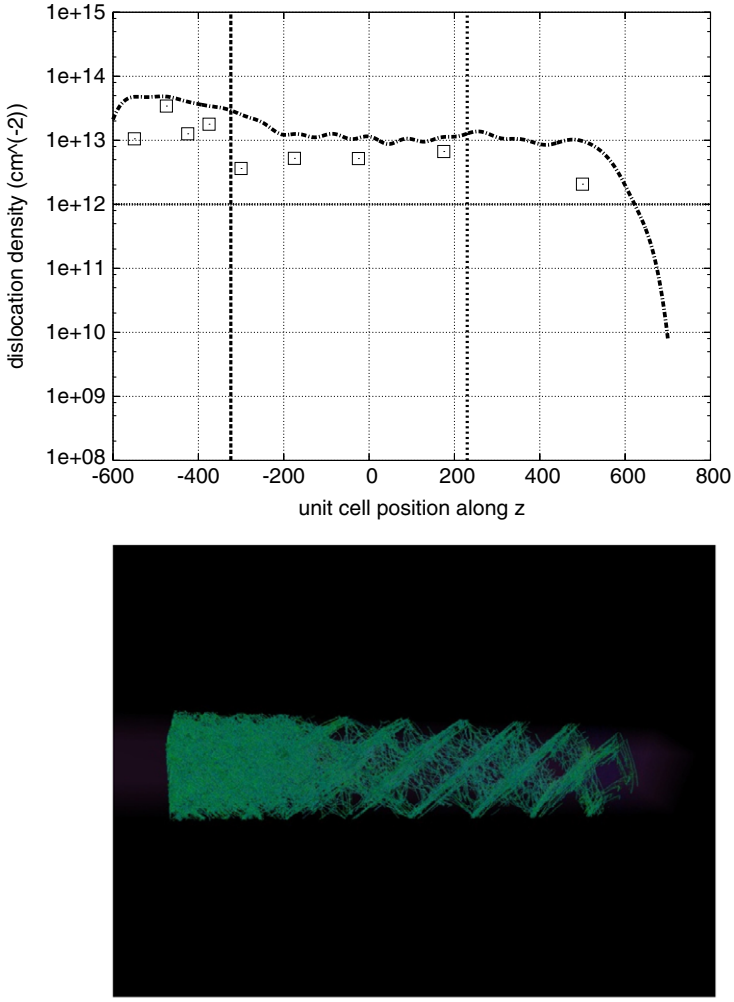

Figure 4. Upper diagram: Squares—dislocation densities inferred from the shifts in the x-ray diffraction peaks as a function of distance in the shock direction in the MD simulation. Positions of the prismatic loops are indicated by the dashed vertical lines. Dot–dashed line—dislocation densities found by direct counting of atoms in the MD simulations. Lower diagram: a snapshot of the corresponding MD simulation [16]

(This figure is in colour only in the electronic version)

front (for this sample, this shear stress is ∼32 GPa). We have found that such high densities of dislocations can have relatively low mobility, as they interlock. This is what happens at early times in the left-hand part of the crystal. However, a prismatic loop acts as a heterogeneous source of dislocations, and can generate new dislocations at shear stresses well below the theoretical shear strength of the material. Thus as the ramp passes over the prismatic loops, dislocations are formed at lower stresses than in the perfect crystal, and such dislocations are also more mobile (for the loops inserted into this sample, the threshold for the activation of the loop was ∼10 GPa). This results in a greater reduction in shear stress for, in fact, fewer dislocations. As noted above, this is not of particular importance for the work contained here, but it gives some insight into why there are different dislocation densities in different regions

of the crystal. What is of significance is that the diffraction technique appears to be capable of resolving these differences.

4. Conclusion

We have identified a method for the calculation of dislocation densities in shock-loaded crystals using *in situ* x-ray diffraction, by comparing the results from the second and fourth diffraction orders in modelled x-ray diffraction from MD simulation of shocked copper crystal. The results are in good agreement with those calculated directly from the MD simulation. As nanosecond diffraction patterns can be obtained experimentally from shocked samples, this work points to the feasibility of making direct *in situ* measurements of dislocation densities in shocked crystals.

Acknowledgments

This work was funded by the UK Engineering and Physical Sciences Research Council (EPSRC) and conducted under the auspices of the US Department of Energy by the University of California Lawrence Livermore National Laboratory (LLNL) under Contract No. W-7405-Eng-48.

References

[1] Johnson Q, Mitchell A C, Keeler R N and Evans L 1969 *Trans. Am. Crystallogr. Ass.* **4** 133
[2] Johnson Q, Mitchell A, Keeler R N and Evans L 1970 *Phys. Rev. Lett.* **25** 1099
[3] Johnson Q and Mitchell A C 1972 *Phys. Rev. Lett.* **29** 1369
[4] Gupta Y M 1977 *J. Appl. Phys.* **48** 5076
[5] Wark J S, Whitlock R R, Hauer A, Swain J E and Solone P J 1987 *Phys. Rev.* B **35** 9391
[6] Wark J S, Whitlock R R, Hauer A A, Swain J E and Solone P J 1989 *Phys. Rev.* B **40** 5705
[7] Rigg P A and Gupta Y M 1998 *Appl. Phys. Lett.* **73** 1655
[8] Loveridge-Smith A *et al* 2001 *Phys. Rev. Lett.* **86** 2349
[9] Zaretsky E 2003 *J. Appl. Phys.* **93** 2496
[10] Orowan E 1940 *Proc. Phys. Soc.* **52** 8
[11] Rosolankova K 2005 Picosecond x-ray diffraction from shock-compressed metals: experiments and computational analysis of molecular dynamics simulations *DPhil Thesis* University of Oxford
[12] Smith C S 1958 *Trans. Metal. Soc. AIME* **212** 574
[13] Meyers M A and Murr L E 1978 *Acta Metall.* **26** 951
[14] Meyers M A 1978 *Scr. Metall.* **12** 21
[15] Holian B L and Lomdahl P S 1998 *Science* **280** 2085
[16] Bringa E M, Duchaineau M, Rosolankova K, Rudd R E, Kalantar D H, Remington B A, Wark J S and Belak J 2006 *Nature Mater.* submitted
[17] Meyers M A, Gregori F, Kad B K, Schneider M S, Kalantar D H, Remington B A, Ravichandran G, Boehly T and Wark J S 2003 *Acta Mater.* **51** 1211
[18] Warren B E 1969 *X-ray Diffraction* (New York: Dover)
[19] Zaretsky E 1995 *J. Appl. Phys.* **78** 3740
[20] Kelchner C L, Plimpton S J and Hamilton J C 1998 *Phys. Rev.* B **58** 11085